Physica A 582 (2021) 126262

Contents lists available at ScienceDirect

Physica A

journal homepage: www.elsevier.com/locate/physa

A cellular automata model for mixed traffic flow considering the driving behavior of connected automated vehicle platoons

Yangsheng Jiang [a,b,d], Sichen Wang [a], Zhihong Yao [a,b,c,d,*], Bin Zhao [a,b], Yi Wang [a,b]

[a] School of Transportation and Logistics, Southwest Jiaotong University, Chengdu, Sichuan 610031, China
[b] National Engineering Laboratory of Integrated Transportation Big Data Application Technology, Southwest Jiaotong University, Chengdu, Sichuan 611756, China
[c] Institute of System Science and Engineering, Southwest Jiaotong University, Chengdu, Sichuan 611756, China
[d] National United Engineering Laboratory of Integrated and Intelligent Transportation, Southwest Jiaotong University, Chengdu, Sichuan 611756, China

ARTICLE INFO

Article history:
Received 9 March 2021
Received in revised form 23 June 2021
Available online 13 July 2021

Keywords:
Mixed traffic flow
Cellular automata model
Connected automated vehicles
Platoon
Maximum platoon size

ABSTRACT

With the development of automated driving technology and communication technology, the emergence of connected automated vehicles (CAVs) will significantly improve traffic efficiency and safety. To study the influence of connected automated vehicles (CAVs) on mixed traffic flow, this study proposes a cellular automata (CA) model of mixed traffic flow considering the driving behavior of the platoon of CAVs. Firstly, three car-following modes, Human-driven vehicle (HDV), Adaptive Cruise Control (ACC), and Cooperative Adaptive Cruise Control (CACC), in mixed traffic flow are analyzed. Secondly, on the bias of the safety distance model and platoon behavior analysis, the acceleration, deceleration, and randomization rules of the cellular automata model of mixed traffic flow are developed. The time step is introduced into the model in the rule design, and the reaction time of the vehicle is considered in the randomization rule. Finally, a numerical simulation is conducted to analyze the fundamental diagram of mixed traffic flow, traffic congestion, and speed volatility under different penetration rates of CAVs. The result shows that (1) the road capacity under the pure CAV environment has increased by 3.24 times compared with the pure HDVs; (2) the maximum congestion reduction percentage can reach 63.36%; and (3) when the penetration rate reaches 80%, the velocity fluctuation decreases significantly. Sensitivity analysis shows that when the penetration rate of CAVs is 100%, the maximum platoon size increase can improve the road capacity. Furthermore, the maximum platoon size has an optimal value in a specific density range.

1. Introduction

Connected automated vehicles (CAVs), as a product combining the automobile industry and emerging technologies, have developed rapidly worldwide in recent years. Compared with human-driven vehicles (HDVs), CAVs can perceive the environment more accurately and realize coordinated control [1,2]. Therefore, the application of CAVs can significantly improve the efficiency of the transportation system. Before the middle of the 21st century, the number of CAVs will exceed 70% of the global car ownership based on the latest research of the Institute of Electronics Engineers (IEEE) [3]. This means that there will be mixed driving on the road of HDVs and CAVs for a long time in the future [4]. Many studies

* Corresponding author at: School of Transportation and Logistics, Southwest Jiaotong University, Chengdu, Sichuan 610031, China.
E-mail address: zhyao@swjtu.edu.cn (Z. Yao).

https://doi.org/10.1016/j.physa.2021.126262
0378-4371/

have been done on the characteristics of mixed traffic flow. Compared with the original traffic flow, the mixed traffic flow can reduce the traffic safety risk [5–7], improve the road capacity [8–10], and improve the stability of the traffic flow when the proportion of CAV reaches a certain range [11–13]. In the mixed traffic flow, CAVs can drive in a platoon via vehicle-to-vehicle communication. Moreover, the platoon composed of CAVs can effectively reduce gasoline consumption and significantly increase the traffic capacity of roads and intersections [14]. Therefore, the study on the characteristics of the mixed traffic flow composed of CAVs' platoon has a great significance.

Cellular automata (CA) can factually simulate complex traffic phenomena by simple rules. In recent years, the CA model has been widely used in transportation research, involving the traffic jams prediction [15], emergency evacuation [16,17], the influence of weather on traffic accidents [18], the prediction of driver's behavior, and other aspects [19,20]. In order to study the characteristics of mixed traffic flow, many existing studies [21–27] use the cellular automata model to describe the micro-driving behavior of vehicles. With the development of CAVs, many scholars have applied the CA model to capture the driving behavior of CAVs. However, the existing research only considers the driving behavior of a single CAV rather than the formation of a platoon when multiple CAVs are in car-following. Therefore, the influence of CAVs' platoon on the characteristics of mixed traffic flow remains to be revealed.

To fill this gap, this study proposes a CA model of mixed traffic flow composed of CAVs' platoon. Firstly, the three car-following modes in mixed traffic flow are analyzed. Then, a CA model of mixed traffic flow considering the driving behavior of CAVs' platoon is developed. Finally, the characteristics of mixed traffic flow and the sensitivity analysis are discussed based on the numerical simulation experiment. Therefore, the main contributions of this work are as follows:

(1) Considering that the V2V communication between the CAVs will make the driving behavior change synchronously, a cellular automata model of mixed traffic flow is developed.

(2) The influence of penetration rate of CAVs on traffic flow is discussed from the aspects of the fundamental diagram, traffic congestion, and speed volatility.

(3) The influence of maximum platoon size of the CAVs on mixed traffic flow is analyzed.

(4) The time step is introduced into the model and the simulation time step is set to 0.1s, which meets the factual conditions that the reaction time of CAV is usually less than 1s.

(5) The reaction time of the vehicle is introduced into the rule of randomization.

The remainder of this study is structured as follows. Section 2 reviews the CA model and its application in CAVs mixed traffic flow is presented. Section 3 proposes the CA model of mixed traffic flow composed of CAVs' platoon. Section 4 discusses the impact of the penetration rate of CAVs on the traffic flow and sensitivity analysis on key parameters based on the simulation experiment. Finally, Section 5 summarizes the research work and puts further improvement forward.

2. Literature review

As an important tool of microscopic traffic flow simulation, cellular automata (CA) can simulate complex traffic phenomena based on some simple rules. Nagel and Schrekenberg [28] proposed the classic NS model. Since then, many scholars have proposed many more realistic models via improving the NS model. Takayasu and Takayasu [29] proposed the TT model based on the rule of slow-start. This model can simulate metastability and hysteresis and can also simulate phase separation in the high-density zone. The BJH model proposed by Benjamin et al. [30] is also based on slow-start rules. Fukui and Ishibashi [31] developed the FI model, which changed the gradual acceleration rule of the vehicle in the NS model and only set the random slowdown on high-speed vehicles. The VDR model proposed by Barlovic et al. [32] rewrote the probability of random slowing down as a function of vehicle speed based on the NS model. Considering the driver wants to drive smoothly and comfortably, Knospe et al. [33] proposed the CD model by introducing the effect of brake lights. Li et al. [34] proposed the VE model based on the speed effect of the leading vehicle. Compared with the previous models, the fundamental diagram of this model is closer to the observed data. Jiang and Wu [35] improved the random slowdown rule based on the CD model. This model argued that the driver would be less sensitive only when the vehicle has stopped for more than a while. The results showed that the MCD model could simulate the synchronous flow and congestion flow well, according to the actual traffic measurement result.

With the development of autonomous driving technology and connected automated vehicle technology, some scholars have gradually studied the mixed traffic flow [36–41]. However, the popularization of CAV will take a long time, so the impact of it can only be analyzed through simulation. Due to the high efficiency of CA model in computer operations, some scholars have applied it to the study of mixed traffic flow in the intelligent transportation environment. These studies involve traffic flow characteristics (including single-lane and multi-lane), intersection traffic control, traffic safety issues, and public transportation.

For the traffic flow characteristics of a single lane, Chen et al. [42] studied the influence of the degree of foresight and ratio of AVs on traffic capacity based on the proposed CA model. The results showed that the road traffic flow can be optimal when the information of the first five vehicles is available to the AV. Besides, there is an optimal ratio of HVs to AVs at a given traffic density. Based on the DHD model proposed by Zhang et al. [43], Hu et al. [44] constructed a CA model that considers speed limits to simulate mixed traffic flow. Vranken et al. [45] introduced AV based on the model of Lee et al. [46] and formulated its rules according to the difference between it and HDV.

For the study of multi-lane traffic flow characteristics, scholars mainly focus on the design of lane changing rules. Yang et al. [47] designed a CA model based on Gipps' safe driving rules. In this model, the parameters of HDV were

Table 1
The comparison of selected literature on CA model research of mixed traffic flow.

Author, Year	Vehicle types	Traffic scene	Considered the platoon of the vehicles
Liu et al. 2017 [48]	(1) HDVs, (2) AVs	Freeway	–
Yang et al. 2017 [47]	(1) HDVs, (2) AVs	Freeway	–
Wu et al. 2017 [53]	(1) AVs	Urban intersection	✓
Zhao et al. 2018 [49]	(1) HDVs, (2) CAVs	Urban intersection	–
Liu et al. 2018 [50]	(1) HDVs, (2) AVs	Freeway	–
Ye and Yamamoto. 2019 [51]	(1) HDVs, (2) CAVs	Freeway	–
Muhammad et al. 2020 [52]	(1) HDVs, (2) HDBs, (3) AVs, (4) ABs	Freeway	–
Hu et al. 2020 [44]	(1) HDVs, (2) AVs	Freeway	–
Chen et al. 2020 [42]	(1) HDVs, (2) AVs	Freeway	–
Vranken et al. 2021 [45]	(1) HDVs, (2) AVs, (3) CAVs	Freeway	–
This study	(1) HDVs, (2) CAVs	Freeway	✓

calibrated with the trajectory data of U.S. Highway 101 collected in the NGSIM project. A two-lane highway was used to simulate different automatic vehicle ratios. The results showed that when the proportion of automatic vehicles increases, the frequency of lane changes decreases, and the capacity of expressways increases. Liu et al. [48] proposed a CA model that considered the lane changing of vehicles. This model was applied to evaluate the impact of mild and aggressive lane changing behavior on traffic flow in a three-lane expressway. The result showed that the traffic capacity and free flow speed would increase as AVs' penetration rate increases. Moreover, intelligent lane changing of AVs on traffic flow was smaller than that of the intelligent car following.

There exist differences between the intersection traffic control mode of mixed traffic flow and conventional traffic flow, since the communication between vehicle and vehicle, vehicle and traffic light under the connected automated environment. Zhao et al. [49] respectively proposed two CA models, the CE-NS model and the CI-NS model, for non-vehicle network intersections and interactions of Internet of Vehicles (IoV). Compared with the CE-NS model, the CI-NS model considered the communication between vehicles and between vehicles and roads in the IoV environment. Conditions such as the speed of the leading vehicle, the dissipation time, and the traffic signal are introduced in the rules. The results showed that the length of the vehicle queue was shorter in the IoV environment. However, connected vehicle technology can significantly optimize the traffic flow at intersections only when the number of CAVs exceeds a certain percentage.

The impact of CAV on traffic safety is one of the significant parts of mixed traffic flow research. Liu et al. [50] employed the CA model to study the accident rate in the mixed traffic flow of AVs and HDVs. The results showed that the safe distance could be set between the AVs and leading vehicles. Ye and Yamamoto [51] used a two-lane CA model to simulate the mixed traffic flow with HDVs and CAVs. Then, the influence of different CAVs' penetration rates on traffic safety was studied based on the simulation results. The frequency of dangerous situations and the value of time-to-collision was used as traffic flow safety evaluation indexes. The result showed that the traffic safety situation would significantly improve with the increase of the CAV penetration rate.

For public transport, Muhammad et al. [52] developed a CA model to study mixed traffic conditions. In this model, the mixed traffic flow contains four kinds of vehicles: AVs, autonomous buses (ABs), HDVs, and human-driven buses (HDBs), and the impact of aggressive lane changing and polite lane changing on traffic flow has also been studied.

The above research shows that the CA model can effectively simulate the mixed traffic flow and be applied to the study of traffic flow characteristics. However, they only considered the behavior of AV or CAV driving in a single-vehicle, and did not consider the situation in which multiple CAVs would form a platoon when they followed. Therefore, the influence of the platoon of CAVs on the characteristics of mixed traffic flow remains to be revealed. Wu et al. [53] established a CA model based on a greedy algorithm for intersections in the AV environment, in which the concept of a platoon was considered, and the platoon of the AVs is used as the control unit. In this intersection, there is no signal light control. Vehicles cross the intersection through the cooperation of V2V and V2I communication. However, since this research mainly focused on the traffic flow at intersections, the primary role of the platoon of the AVs was to control the traffic flow as the basic unit when vehicles pass through the intersection. Besides, in this model, only AVs are included in the traffic flow. Therefore, this study aims to propose a single-lane CA model for mixed traffic flow to study the influence of the CAVs platoon on the characteristics of mixed traffic flow. Compared with the model proposed by Jiang et al. [54], the time step is introduced into the CA model in this study, and the simulation step is set to 0.1s considering that the reaction time of the CAV is less than 1s. At the same time, the reaction time is introduced into the randomization rule, and the influence of maximum platoon size on traffic flow is analyzed. Table 1 summarizes the detailed comparison of the CA model research of mixed traffic flow in the intelligent network environment.

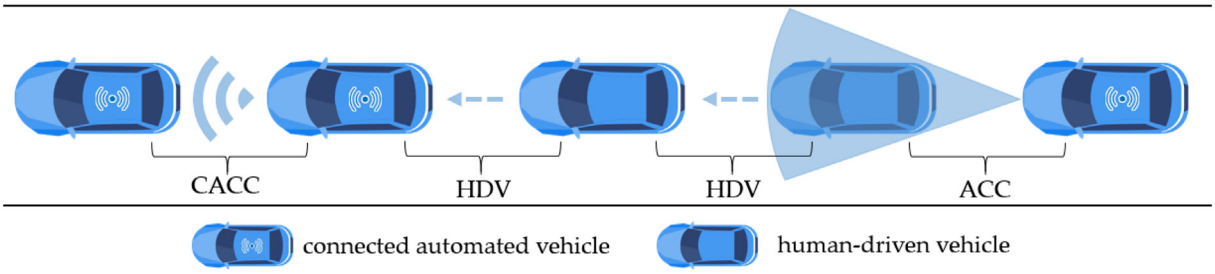

Fig. 1. Car-following modes in mixed traffic flow.

3. Methodology

3.1. Car following mode

When there are both CAVs and HDVs on the road, the car-following modes of different vehicles can be described in Fig. 1. According to the analysis, there are three car-following modes: human-driven vehicle (HDV), adaptive cruise control (ACC), and cooperative adaptive cruise control (CACC).

3.1.1. Human-driven vehicles mode

As shown in Fig. 1, the HDV car-following mode includes two situations. In the first case, the follower is an HDV, and the leader is a CAV. In the second case, the follower and the leader are both HDVs. When the driving behavior of the leading vehicle changes, the human driver needs time to perceive, recognize and judge the change in the driving state of the leading vehicle before taking measures; this time is called reaction time in this study. In this mode, the reaction time is determined by the driver. Besides, the vehicle may produce random deceleration because of uncertain factors such as the driver's mentality.

3.1.2. Adaptive cruise control mode

In ACC car-following mode, the follower is a CAV, and the leader is an HDV. The follower uses the on-board sensing system to obtain the status information of the leader. Therefore, the follower can quickly capture the change of the leader's behavior and take corresponding measures. The reaction time is the processing time of the on-board sensing system, which is shorter than that of the HDV mode.

3.1.3. Cooperative adaptive cruise control mode

In the CACC car-following mode, the follower and the leader both are CAVs. The follower can achieve the synchronous change of the leader's driving behavior via V2V communication, so it can be regarded as a 'vehicle platoon'. The reaction time in this mode is the communication and braking delay of the CACC system. Therefore, its value is far less than that of HDV mode, usually taken as 0.

3.2. Cellular automaton model

The CA model can simulate complex traffic phenomena based on some simple rules. For the characteristics of the above three car-following modes, corresponding rules are developed respectively. Finally, the CA model of mixed traffic flow is obtained.

To distinguish different car-following modes, let α_n, β_n, and γ_n are 0–1 variable used to judge whether the car-following mode of the vehicle n is HDV, ACC, and CACC, respectively. They are determined by

$$\alpha_n = \begin{cases} 1, & \text{if the car following mode of the vehicle } n \text{ is HDV} \\ 0, & \text{else,} \end{cases} \tag{1}$$

$$\beta_n = \begin{cases} 1, & \text{if the car following mode of the vehicle } n \text{ is ACC} \\ 0, & \text{else,} \end{cases} \tag{2}$$

$$\gamma_n = \begin{cases} 1, & \text{if the car following mode of the vehicle } n \text{ is CACC} \\ 0, & \text{else,} \end{cases} \tag{3}$$

$$\alpha_n + \beta_n + \gamma_n = 1. \tag{4}$$

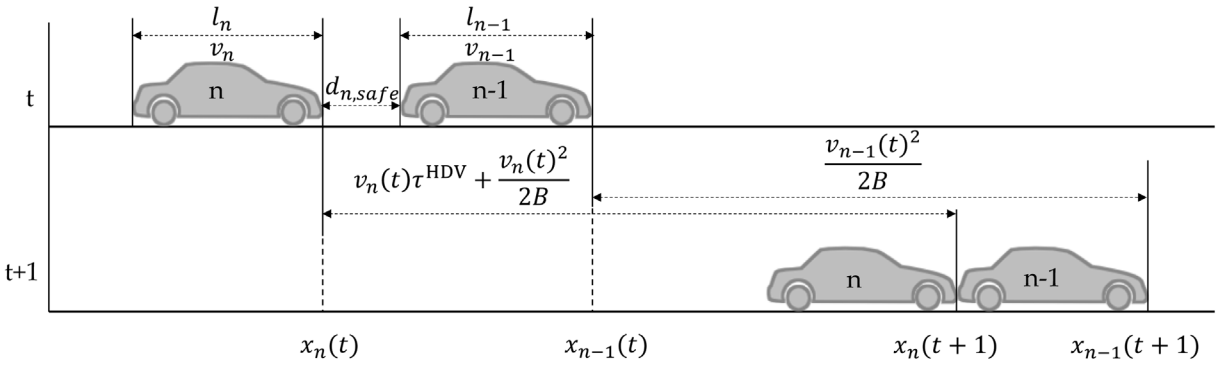

Fig. 2. The schematic diagram of safe distance.

Then, safety distance is introduced into the design of rules [47]. The concept of safe distance is based on the viewpoint of the Gipps model [55], rewriting the minimum stopping distance in the Gipps model and considering the characteristics of the CA model comprehensively. It is the minimum distance that the follower does not collide with the leader vehicle when the leader vehicle brakes suddenly. The safety distance of the vehicle defined in this way can ensure that the vehicle is safe in all cases. Assuming that both vehicles n and $n-1$ are HDV, the schematic diagram of safe distance is shown as Fig. 2. In mixed traffic flow, the calculation method is not single. For vehicles in HDV mode, the safety distance is $v_n(t)\,\tau^{\mathrm{HDV}} + \frac{v_n(t)^2 - v_{n-1}(t)^2}{2B}$. The main difference between ACC mode and HDV mode is the reaction time of the follower. Therefore, for vehicles in ACC mode, the safety distance is $v_n(t)\,\tau^{\mathrm{CAV}} + \frac{v_n(t)^2 - v_{n-1}(t)^2}{2B}$. The vehicles in CACC mode can achieve V2V communication. The follower can extract the driving behavior of the leader at the next time steps in advance. In an emergency, the leading vehicle will immediately notify the following vehicle of braking measures to brake simultaneously. Therefore, the safety distance of vehicles with CACC mode is minimal, which is set as a constant d_s^{CACC} in this study. Compared with variable distance, constant safety distance requires communication between vehicles to ensure string stability [56]. Therefore, that it is feasible to set a constant safety distance when vehicles can communicate with each other. This is similar to the characteristics of the vehicle in CACC mode, that the vehicle can communicate with the leading vehicle in real-time. In addition, the constant safe distance is In addition, the constant safe distance is more suitable for close formation platforms which keep a small space between vehicles [57]. The safe distance of CACC vehicles also means the distance that vehicles need to maintain when forming a platoon in this study. It is similar to the concept of close-formation platoons. Therefore, the safety distance of CACC vehicles is set to be constant. To sum up, the safe distance between adjacent vehicles in mixed traffic flow can be determined by

$$d_{n,safe} = v_n(t)\left(\alpha_n \tau^{\mathrm{HDV}} + \beta_n \tau^{\mathrm{CAV}}\right) + (\alpha_n + \beta_n)\left(\frac{v_n(t)^2 - v_{n-1}(t)^2}{2B}\right) + \gamma_n d_s^{\mathrm{CACC}}, \tag{5}$$

where $d_{n,safe}$ is the safe distance between the vehicle n and vehicle $n-1$. $v_n(t)$ is the speed of the vehicle n at time t (m/s). τ^{HDV} and τ^{CAV} are the reaction time (s) of the HDV and the CAV, respectively. B is the maximum deceleration of the vehicle (m/s^2). d_s^{CACC} is the safety distance of vehicles with CACC mode.

As shown by Eq. (5), the safe distance is a polynomial function of speed in this study. Compared with the linear relationship between speed and the constant time gap, this method can not only ensure the safety of vehicles in any case, but also shorten the safety distance when necessary. Take the vehicle in HDV mode as an example, $\alpha_n = 1$ and its safe distance is $d_{n,safe} = v_n(t)\,\tau^{\mathrm{HDV}} + \frac{v_n(t)^2 - v_{n-1}(t)^2}{2B}$. In this case, there are also three situations for the safe distance. First, when $v_n(t) < v_{n-1}(t)$, the second term in the formula $\frac{v_n(t)^2 - v_{n-1}(t)^2}{2B} < 0$. In this case, the safe distance $d_{n,safe}$ is smaller than $v_n(t)\,\tau^{\mathrm{HDV}}$ because the speed of the following vehicle is slower. Compared with the linear relationship between speed and the constant time gap, this method can shorten the safe distance under the condition of ensuring safety, which is more conducive to improving road capacity and average vehicle speed. Second, when $v_n(t) = v_{n-1}(t)$, the second term in the formula $\frac{v_n(t)^2 - v_{n-1}(t)^2}{2B} = 0$. The safe distance $d_{n,safe} = v_n(t)\,\tau^{\mathrm{HDV}}$, when the speeds of both the proceeding and following cars are stable and equal. Third, when $v_n(t) > v_{n-1}(t)$, the second term in the formula $\frac{v_n(t)^2 - v_{n-1}(t)^2}{2B} > 0$. In this case, the required safe distance $d_{n,safe}$ is larger than $v_n(t)\,\tau^{\mathrm{HDV}}$ because the speed of the following vehicle is faster. This method can ensure the absolute safety of the vehicle, compared with simply defining the safety distance as the linear relationship between speed and the constant time gap.

Based on the safe distance of different car-following modes, the acceleration, deceleration, randomization, and position update rules of the CA model of mixed traffic flow are proposed as follows.

3.2.1. Acceleration

For HDV and ACC modes, when the distance d_n between vehicle n and its leading vehicle $n-1$ is greater than the safety distance $d_{n,safe}$, vehicle n will accelerate due to the pursuit of higher speed. To avoid traffic accidents and obey the speed limit, the speed of vehicle n at the next time step is the minimum of $v_n(t)+\alpha_n\Delta t$, V_{max}, and $d_n/\Delta t$.

CACC mode allows real-time communication between vehicles, compared with HDV and ACC modes. Therefore, the vehicle in the CACC mode can adjust the speed by obtaining the speed at the next moment of the leading vehicle. The above analysis shows that the vehicles in CACC mode can be driven in the form of a platoon, and the vehicles in the same platoon can maintain a stable distance and the same driving behavior. When the distance between vehicle n and vehicle $n-1$ is greater than the safe distance, vehicle n will adjust its speed to form a platoon with the leading vehicle as soon as possible. In this case, the speed of vehicle n at the next moment is the minimum of $v_n(t)+a\Delta t$, V_{max}, and $d_n/\Delta t+v_{n-1}(t+\Delta t)-d_{n,safe}/\Delta t$. The $d_n/\Delta t+v_{n-1}(t+\Delta t)-d_{n,safe}/\Delta t$ is the speed required by vehicle n to drive the platoon in the next time step. Therefore, the form of the acceleration rule is shown as follows.

$$v_n(t+\Delta t)=(\alpha_n+\beta_n)\min\left(v_n(t)+a\Delta t, V_{max}, d_n/\Delta t\right)+\gamma_n\min\left(v_n(t)+a\Delta t, V_{max}, d_n/\Delta t, d_n/\Delta t+v_{n-1}(t+\Delta t)-d_n\right. \quad (6)$$

where,

$$d_n=x_{n-1}(t)-x_n(t)-l_{n-1},$$

where Δt is the time step (s). $v_n(t+\Delta t)$ is the speed of vehicle n at time $t+\Delta t$ (m/s). a is the acceleration of the vehicle (m/s^2). V_{max} is the maximum speed of the vehicle (m/s). d_n is the distance between vehicle n and vehicle $n-1$ (m). $v_{n-1}(t+\Delta t)$ is the speed of vehicle $n-1$ at time $t+\Delta t$ (m/s). $d_{n,safe}$ is the safe distance of vehicle n (m), which can be obtained by Eq. (5). $x_{n-1}(t)$ is the position of vehicle $n-1$ at time t (m). $x_n(t)$ is the position of vehicle n at time t (m). l_{n-1} is the length of vehicle $n-1$ (m).

3.2.2. Deceleration

When the distance d_n between the vehicle n and the vehicle $n-1$ is less than or equal to the safe distance $d_{n,safe}$, the vehicle will decelerate to ensure driving safety. The d_n of vehicles in CACC mode will not be less than the $d_{n,safe}$ because of the particularity of acceleration rules. When d_n is equal to $d_{n,safe}$, the two vehicles become stable platoon with the same driving behavior (acceleration and deceleration). Therefore, the speed of vehicle n at the next moment is $v_{n-1}(t+\Delta t)$. The form of the deceleration rule is shown as follows.

$$v_n(t+\Delta t)=(\alpha_n+\beta_n)\min\left(v_n(t), d_n/\Delta t\right)+\gamma_n v_{n-1}(t+\Delta t), \text{ if } d_n\le d_{n,safe}. \quad (7)$$

3.2.3. Randomization

Taking into account the unstable factors of the human driver, the randomization probability p_{slow} is introduced. Vehicles will slow down according to the randomization probability. A 0–1 variable η_n^t is defined here to indicate whether the vehicle slows down randomly. Besides, in the same reaction time, the random slowdown state of the vehicle is the same. Re-value η_n^t at the initial time of the next reaction time. That is, re-judge the random slowing state of the vehicle. In particular, since there are no unstable factors in CAVs, there is no randomization process for vehicles in ACC mode and CACC mode. The randomization rule of vehicle n is obtained as Eqs. (8) and (9).

$$\eta_n^t=\begin{cases}1, & \text{if } rand\le p_{slow} \text{ and } t \bmod \tau^{\mathrm{HDV}}=0\\ 0, & \text{if } rand>p_{slow} \text{ and } t \bmod \tau^{\mathrm{HDV}}=0\\ \eta_n^{t-\Delta t}, & \text{other,}\end{cases} \quad (8)$$

$$v_n(t+\Delta t)=\max\left(v_n(t)-\alpha_n\eta_n^t b\Delta t, 0\right), \quad (9)$$

where b is the random deceleration of the vehicle (m/s^2). p_{slow} is the randomization probability.

3.2.4. Position update

After the next time step's speed is updated, the position of the vehicle is updated by Eq. (10).

$$x_n(t+\Delta t)=x_n(t)+v_n(t+\Delta t)\cdot\Delta t. \quad (10)$$

4. Numerical simulation

4.1. Simulation setting

Based on the proposed model, a numerical simulation is used to study the characteristics of the mixed traffic flow on a single-lane freeway. In the numerical simulation, the lane consisting of 4000 cells, and each cellular length take 0.01 m, so the length of the road is $L=400$ m. The simulation time step is set to 0.1 s, and the total steps are 2000. The final 1000 steps are recorded to investigate the traffic flow characteristics. The simulation uses the periodic boundary. In the initial state, the vehicles distribute on the road evenly, and the speed generates randomly. The length of the vehicles is 500 cells

Table 2
Parameters for the simulation.

Parameter	Value
V_{max}	350 cells/step (35 m/s)
a	20 cells/step^2 (2 m/s^2)
b	30 cells/step^2 (3 m/s^2)
B	50 cells/step^2 (5 m/s^2)
p_{slow}	0.2
τ^{HDV}	20 steps (2 s)
τ^{CAV}	6 steps (0.6 s)
d_s^{CACC}	50 cells (0.5 m)

(5 m). The speed limit is $V_{max} = 350$ cells/step (126 km/h). The general acceleration, random deceleration, and maximum deceleration of the vehicles are $a = 20$ cells/step^2 (2 m/s^2), $b = 30$ cells/step^2 (3 m/s^2), and $B = 50$ cells/step^2 (5 m/s^2), respectively. The randomization probability of the HDVs is set to be 0.2. The reaction time of the HDVs and the CAVs are often assumed to be around 1.6–2.5 s and 0.5–0.75 s [58]. Therefore, the reaction time of the HDVs and CAVs are set to 20 steps (2 s) and 6 steps (0.6 s) in the simulation, respectively. The safe distance of the vehicles in CACC mode is d_s^{CACC}. Different values of d_s^{CACC} will affect the simulation results, the influence of d_s^{CACC} will be analyzed later. The value of d_s^{CACC} can be a fixed distance or a distance corresponding to the fixed time headway and its value needs to be set according to the Cooperative Adaptive Cruise Control system. In this study, the value of d_s^{CACC} is a fixed distance, which is set to be 50 cells (0.5 m) in this simulation. The values of parameters in the numerical simulation are shown in Table 2. In order to study the influence of the penetration rate of CAVs on the characteristics of mixed traffic flow, the penetration rates are set to 0%, 20%, 40%, 60%, 80%, and 100%.

4.2. Results and discussions

4.2.1. Fundamental diagram

As shown in Fig. 3, the fundamental diagram is affected by the penetration rate of CAVs significantly. Fig. 3(a) indicates that the average speed of the vehicles increases with the traffic density decreasing. Besides, the average speed of the vehicles will rise significantly with the increase of penetration rate under the same traffic density. Fig. 3(b) shows that with the rise of the penetration rate, the road capacity is increasing. When the penetration rate increases from 60% to 80%, the road capacity increases from 1.97 times to 3.24 times that of only HDVs. This means that the road capacity increases with the rise of the penetration rate of CAVs. When the penetration rate is 100%, the traffic flow increases linearly with the traffic density, and the average speed is equal to the maximum speed. The vehicles are free-flow before the traffic density reaches saturation. This is because the CAVs will not decelerate randomly and will adjust the speed to form a platoon continuously. The vehicles that do not form a platoon will continue to accelerate and catch up with the previous platoon until they join it or reach the maximum speed. Finally, one or more vehicle platoons will be formed at the maximum speed after stabilizing all vehicles. The road capacity is only affected by the critical traffic density when all the vehicles are CAVs. Therefore, the increase of CAVs' penetration rate is conducive to the improvement of road capacity.

Fig. 4 shows the headway of vehicles in different penetration rates at the traffic density of 60 vehicles/km and the 1500th time step. As shown in Fig. 4(a)–(b), in the case of a low penetration rate, it is impossible to form a large-scale platoon on the road because most of the leaders of the CAVs are HDVs. However, the platoon system still exists on the road under conditions of low penetration rate. Fig. 4(c)–(d) shows that as the penetration rate increases, one or more platoons will form on the road. The vehicles in the platoon maintain a small distance and realize synchronous changes in driving behavior. When the penetration rate of CAVs reaches 100%, all the vehicles are driven in platoon after stabilization. However, considering the limitation of the maximum speed, the latter platoon cannot catch up with the proceeding platoon. Eventually, there will be one or more platoon driving at maximum speed on the road.

4.2.2. Trajectory–velocity diagram analysis

Fig. 5 shows the trajectory of vehicles under different CAVs' penetration rates at the traffic density of 100 vehicles/km. The congested area is marked by different colors. The darker the color on the figure, the lower the vehicle speed, which means the greater the degree of traffic congestion. It can be seen from Fig. 5(b)–(e) that with the increase of penetration rate, the trajectory of vehicles becomes inclined, and the congestion area becomes smaller. Moreover, the trajectory of the vehicles indicates that some vehicles are densely distributed, and their driving behaviors are kept in synchronization. As shown in Fig. 5(f), when the penetration rate of CAVs is 100%, the traffic congestion only exists in the region of the initial period, and there is no traffic congestion in other areas. The main reason is that the initial speed is randomly generated, and the vehicles adjust rapidly in the process of driving to form one or more platoons. After the formation of the platoons, the vehicles on the road are operating at maximum speed.

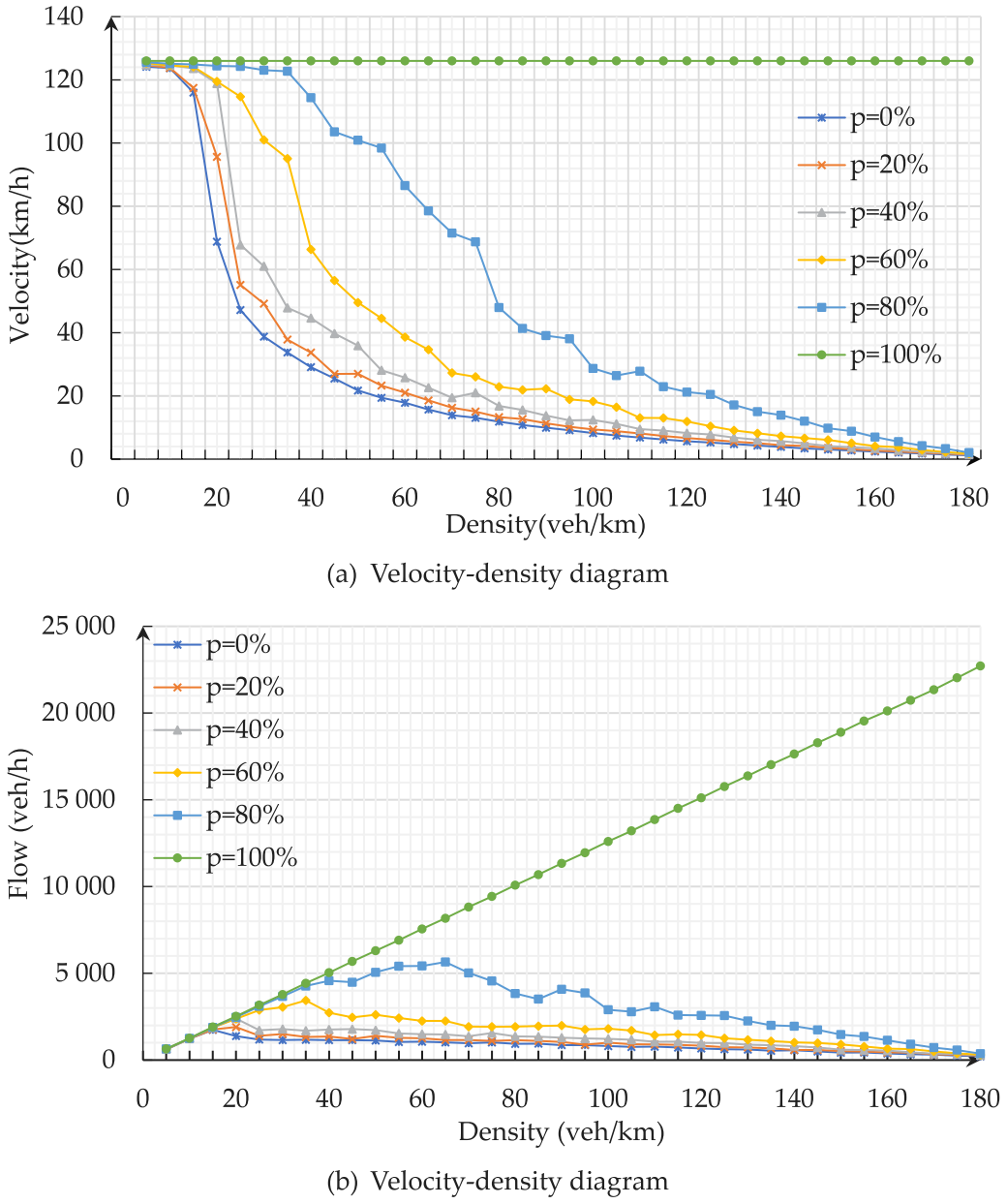

Fig. 3. The fundamental diagram of different penetration rates.

4.2.3. Congestion analysis

To describe traffic congestion quantitatively, the proportion of congested vehicles is used to reflect the traffic congestion [47]. The calculation formula is as follows.

$$CR = \frac{n}{\Delta T \cdot N}, \tag{11}$$

where n is the number of vehicles with severe congestion, and the vehicles with speed lower than 10 km/h are defined as vehicles with severe congestion. ΔT is the simulation time steps, and N is the total number of vehicles.

Fig. 6 shows that the proportion of traffic congestion increases with the rise of traffic density. In the case of the penetration rate of CAVs is 0%, the traffic density of 20 vehicles/km is the threshold at which congestion begins. In contrast, when the penetration rate is 80%, the threshold traffic density becomes 40 vehicles/km.

Further, the traffic density of 100 vehicles/km is selected as an example, we calculate the percentage of traffic congestion reduction under different penetration rates of CAVs. The results are shown in Table 3.

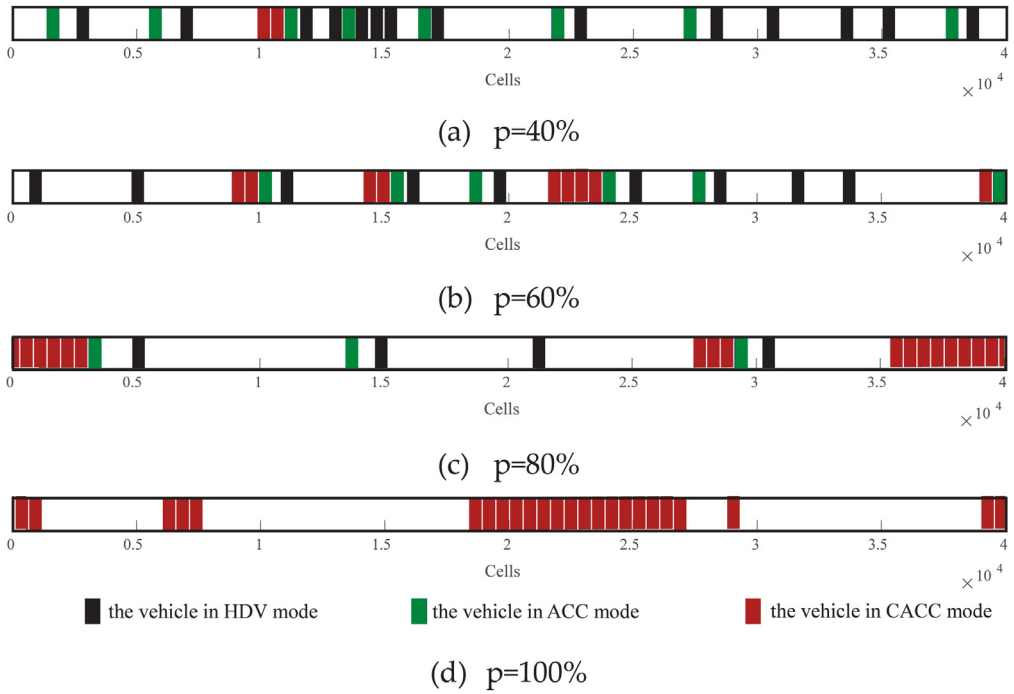

Fig. 4. Vehicles' headway of different CAVs' penetration rates.

Table 3
Traffic congestion reduction percentage of different penetration rates (100 vehicles / km)

Penetration rates	Traffic congestion ratio	Traffic congestion reduction percentage
0%	66.07%	0.00%
20%	61.92%	6.28%
40%	51.32%	22.32%
60%	39.98%	39.49%
80%	24.22%	63.36%
100%	0.00%	100.00%

Table 3 indicates that when the traffic density is 100 vehicles/km and the penetration rate is 80%, the traffic congestion is reduced by 63.36% compared with pure HDVs. In particular, Fig. 6 shows that when the penetration rate is 100%, the traffic congestion ratio at all traffic densities is equal to 0%. The main reason is that all vehicles are running in a free flow state after the CAVs have formed a stable platoon. Combined with the above analysis, it can be concluded that the large-scale application of CAVs can effectively alleviate traffic congestion.

In this study, the CAV does not significantly relieve road congestion when the penetration rate is low, compared with other studies [59,60]. There are two main reasons for this phenomenon. First, other literature mainly studies the adaptive cruise control strategy, and optimizes the control strategy to avoid congestion, where the optimization effect is significant despite the low penetration rate. Second, the HDV reaction time set in the simulation environment in this study takes a more significant value. Therefore, in the process of random slowing down, the selected vehicle will decelerate continuing. After the random slowdown process, there are many vehicles with speeds less than 10 cells/step or even 0 cells/step, which will cause serious congestion. Although CAV in a small number can alleviate the congestion, it still takes a long time to dissipate the congestion.

4.2.4. Speed volatility analysis

Fig. 7(a) shows that when the penetration rate is low, the speed of the vehicle changes drastically during driving, which means the instability of the vehicle movement. At this point, the frequent acceleration and deceleration of the vehicle will lead to greater fuel consumption and exhaust emissions. Besides, Fig. 7(b)–(d) indicates that with the increase of penetration rate, the vehicle speed rises significantly, and the volatility of speed decreases gradually. This means CAVs can reduce fuel consumption and exhaust emissions significantly. The main reason is that the CAVs will not be affected by the driver decelerating randomly like the HDVs.

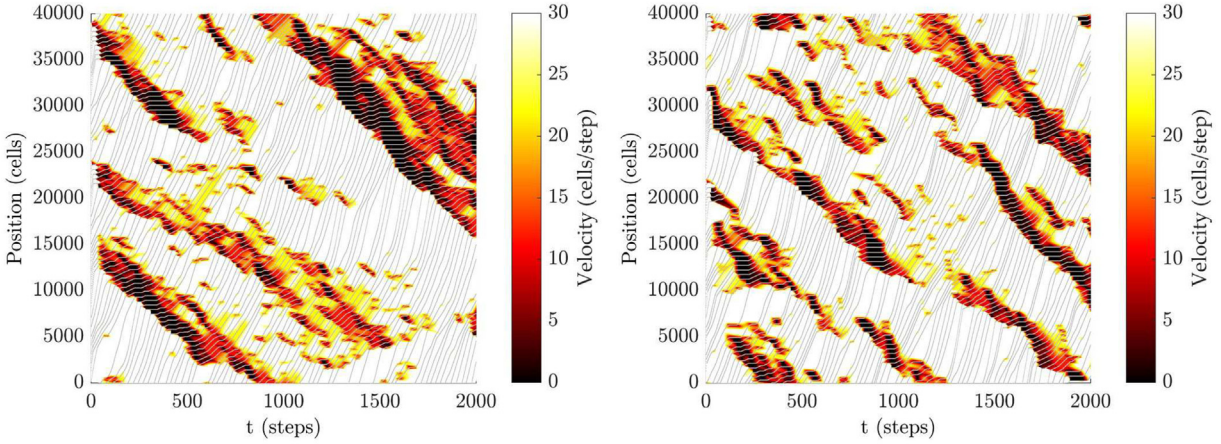

(a) p=0% (b) p=20%

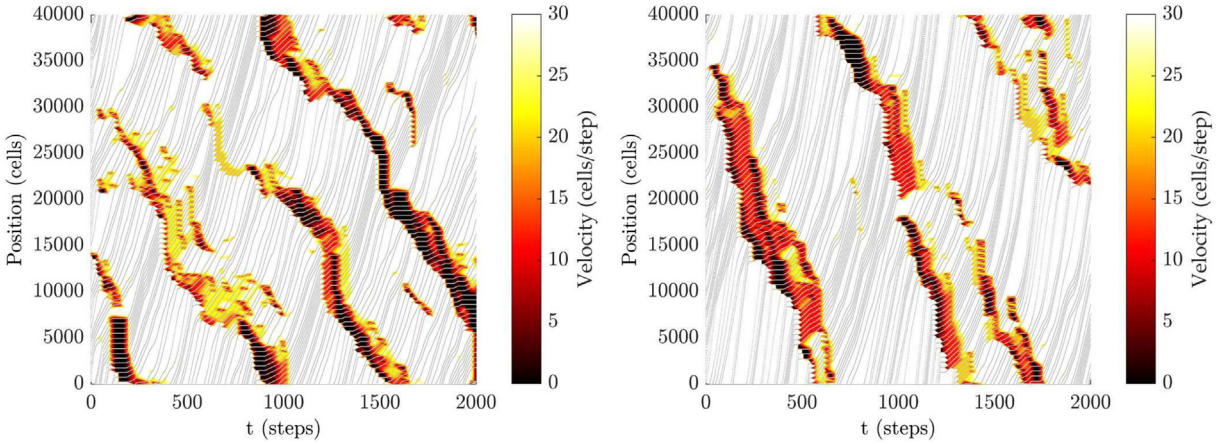

(c) p=40% (d) p=60%

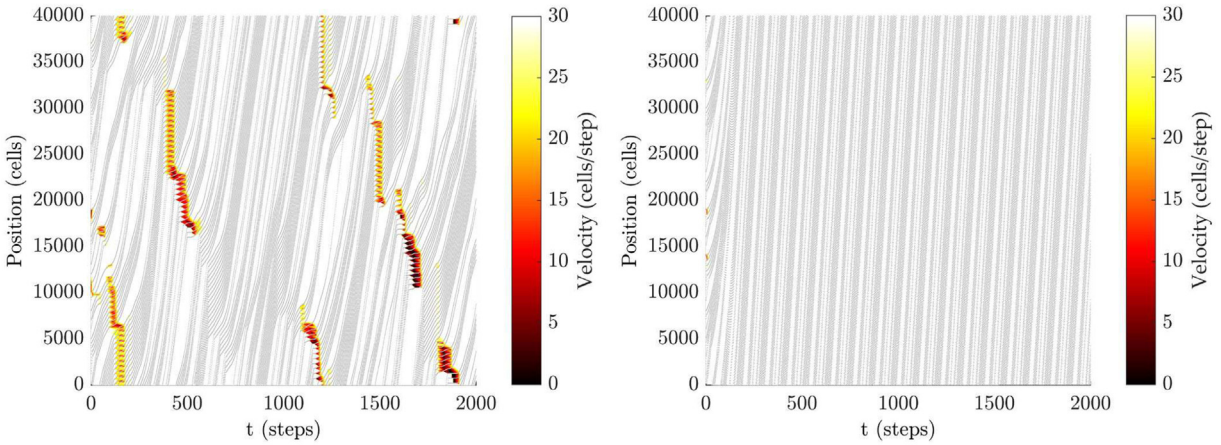

(e) p=80% (f) p=100%

Fig. 5. The trajectory–velocity diagram of different penetration rates of CAVs.

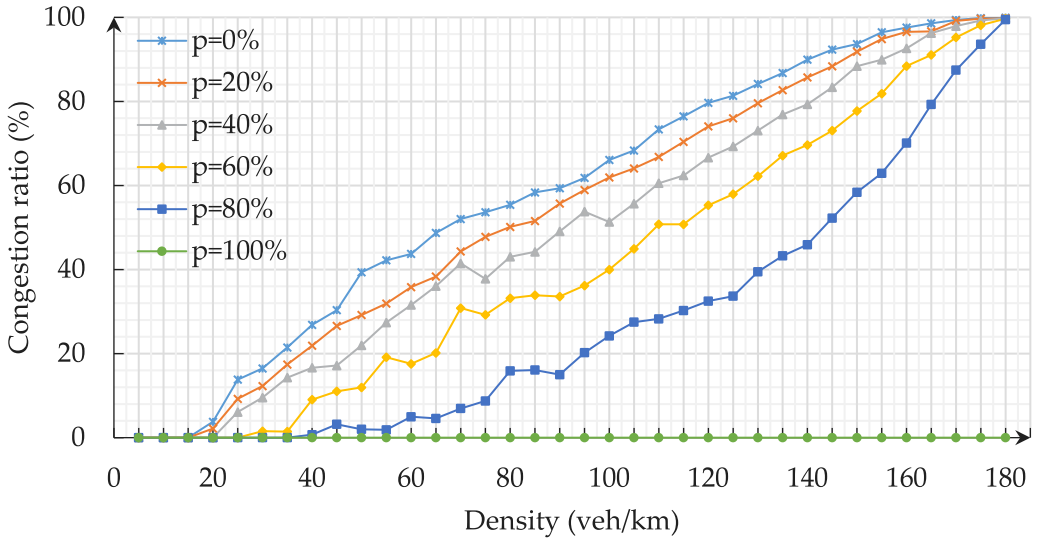

Fig. 6. Congestion ratio vs. traffic density of different penetration rates.

4.3. Sensitivity analysis

In this study, the safe distance of the vehicle in CACC mode (d_s^{CACC}), the reaction time of HDVs and CAVs (τ^{HDV} and τ^{CAV}), maximum platoon size are the most critical parameters. To further analyze the impacts of these parameters, three sensitivity analysis is performed.

4.3.1. The safe distance of the vehicles in CACC mode

A reasonable safety distance during driving can ensure the safety of the vehicle. Excessive safety distance may waste traffic capacity. On the contrary, a small safety distance may cause more accidents. Because V2V communication can be used between vehicles in CACC mode, the safety distance is much shorter than that of vehicles in the other two car-following modes. However, it still needs to maintain the safety distance of CACC mode. The different value of d_s^{CACC} may affect traffic flow parameters. In the sensitivity analysis, the values of d_s^{CACC} are set as 0.2 m, 0.5 m, and 1 m, respectively. Firstly, the penetration rate is determined to be 80% to study the influence of different d_s^{CACC} on the density-flow curve. Then, the influence of d_s^{CACC} on road capacity is studied separately for different penetration rates of CAVs. The sensitivity analysis result is shown in Fig. 8.

Fig. 8(a) shows that when the traffic density is low, the value of d_s^{CACC} has no significant impact on traffic flow. However, when the traffic density is greater than or equal to the critical traffic density, the value of d_s^{CACC} has a significant impact on the traffic flow. A smaller d_s^{CACC} can increase the number of vehicles passing by per unit time at the same traffic density. This is because d_s^{CACC} refers to the safe distance between vehicles in CACC mode, which is the minimum distance. The vehicles in the platoon maintain this distance, and the change of d_s^{CACC} will affect the headway of them. In the case of low traffic density, the number of vehicles per unit length of the road is fewer, and the headway between platoons and between vehicles which not belong to the platoons is large. The changes of d_s^{CACC} in a small range have limited impact on the average headway of the vehicle. Therefore, when the traffic density is low, the change of the value of g_s^{CACC} basically does not affect the value of traffic flow. On the contrary, when the traffic density is higher, the change of d_s^{CACC} will significantly affect the average headway because of the smaller headway of other vehicles. Therefore, in the case of high traffic density, the traffic flow will decrease with the increase of d_s^{CACC} value.

As shown in Fig. 8(b), as the penetration rate increases, the change of d_s^{CACC} has an increasingly significant impact on capacity. Additionally, the smaller the d_s^{CACC}, the larger the capacity. In the case of a low penetration rate, there are fewer CAVs, even fewer vehicles in CACC mode. The change of d_s^{CACC} only affects a small proportion of vehicles, so the impact on the overall traffic is minimal. As the penetration rate increases, the proportion of vehicles in CACC mode increases. Therefore, when the penetration rate is high, the change of the value of d_s^{CACC} has a significant impact on the road capacity.

4.3.2. The reaction time of HDVs and CAVs

The magnitude of the reaction time is one of the critical differences between CAVs and HDVs. The reaction time of HDVs (τ^{HDV}) is mainly affected by human drivers, while the reaction time of CAVs (τ^{CAV}) refers to the processing time of the on-board sensing system. Generally, the reaction time of the latter is less than that of the former. In the sensitivity analysis, the density is set as 60 veh/km, τ^{HDV} varies from 1.6 s to 2.5 s with increments of 0.1 s, and τ^{CAV} varies from 0.5 s to 0.75 s with increments of 0.05 s. The sensitivity analysis result is shown in Fig. 9.

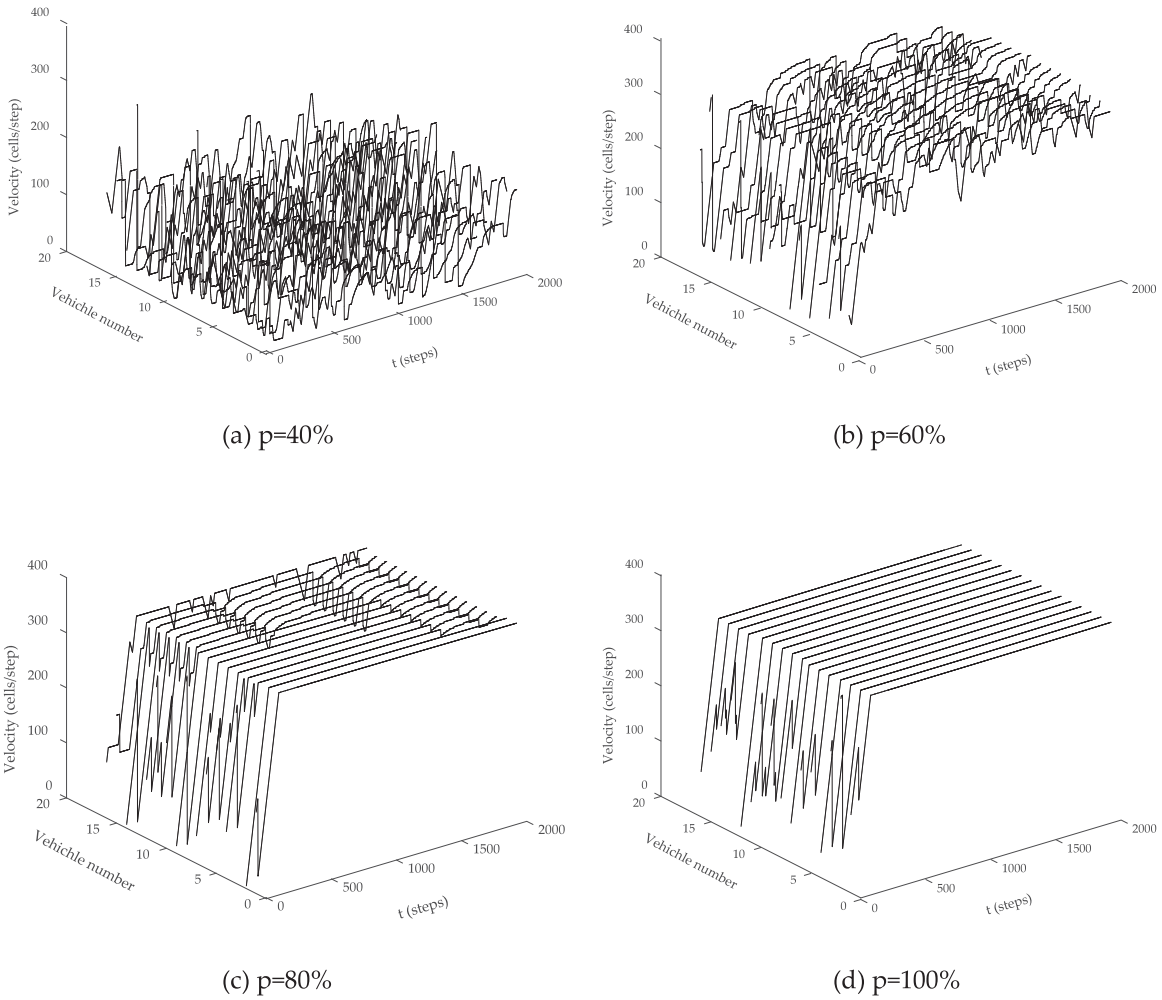

Fig. 7. The speed volatility of different penetration rates.

Fig. 9 shows that the value of τ^{HDV} and τ^{CAV} have significant differences in the degree of influence on the average speed under different penetration rates of CAVs. As shown in Fig. 9(a)–(e), regardless of the penetration rate of the CAVs, the average speed will decrease significantly with the increase of the value of τ^{HDV}. There are two main reasons. Firstly, when the penetration rate is low, HDVs are affected by τ^{HDV} account for a relatively high proportion. τ^{HDV} and the required safety distance of the vehicle change in the same direction according to Eq. (5). This means that when other conditions are equal, more vehicles will accelerate at the next time step. Therefore, the average speed will decrease significantly with the prolong of τ^{HDV}. Secondly, HDVs are affected by the random slowdown process. The random slowdown effect received by a certain vehicle will be continuously transmitted to other vehicles as it moves, causing the speed volatility of other vehicles. In this study, the reaction time of HDVs is considered in the random slowdown rules. In the same period of reaction time, the random slowdown state of the vehicle is identical, and the speed will decrease evenly. Therefore, when τ^{HDV} is prolonged, the vehicle will decelerate more greatly in a random slowing down process. Other vehicles located behind the vehicles, which in a random slowdown state, will also adjust the speed to avoid accidents. Compared with the slight deceleration, the sharp deceleration has a more significant impact on the rear vehicles, even affecting the stability of the vehicle speed of the entire road system. Therefore, even if there are few HDVs (the penetration rate of CAVs is high), the τ^{HDV} still have a significant impact on the average speed with the existence of random slowdown.

Fig. 9(a)–(b) indicates that the average speed of vehicles with a low penetration rate is hardly affected by τ^{CAV}. The reason is that the number of CAVs affected by τ^{CAV} is small in this circumstance, which implies that the influence of τ^{CAV} has limitation. As shown in Fig. 9(c)–(e), the influence of τ^{CAV} is gradually significant as the penetration rate increases.

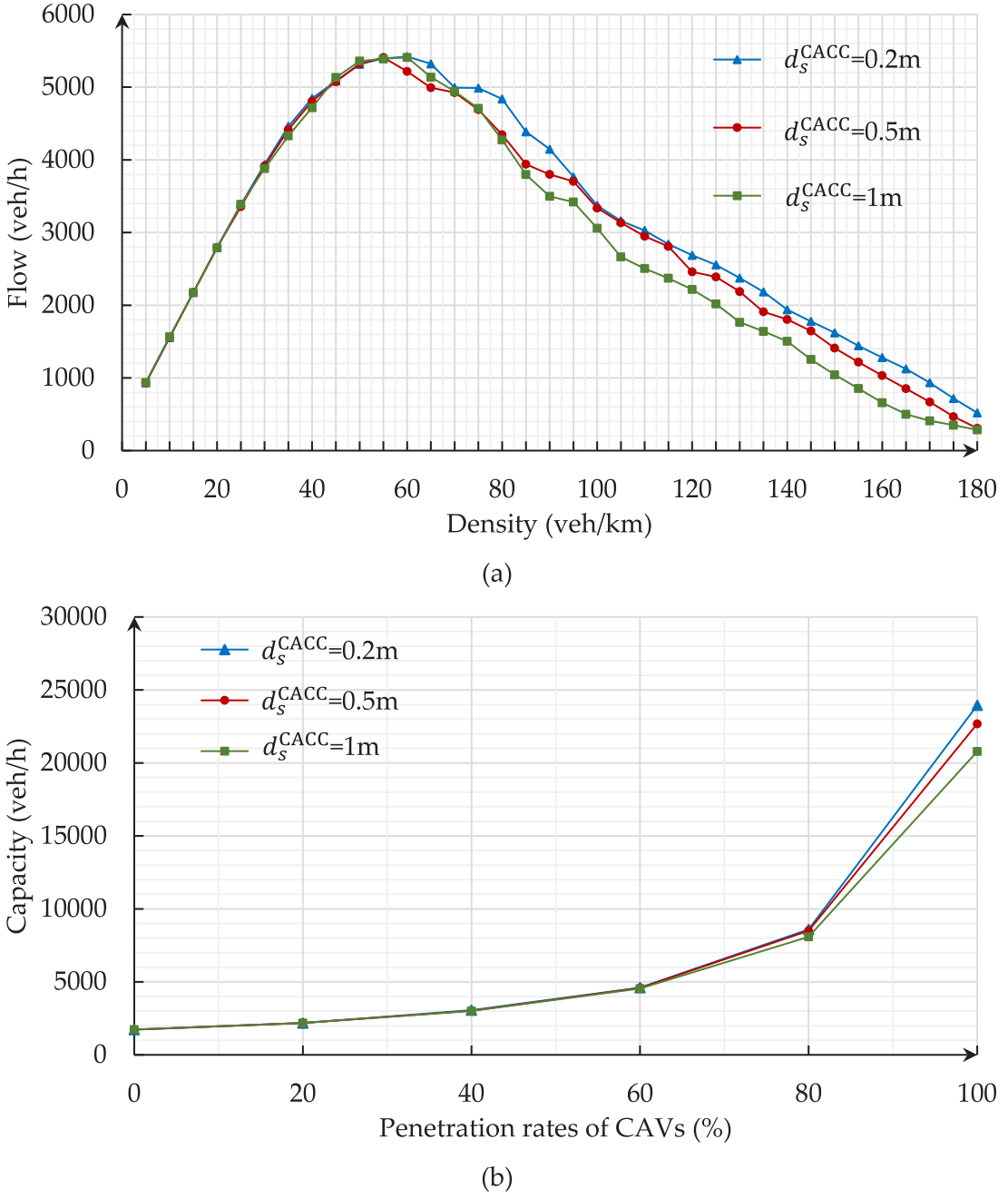

Fig. 8. Sensitivity analysis on the safe distance of the vehicle in CACC mode.

The decrease of τ^{CAV} will result in the decrease of the safety distance required by the vehicle, and more vehicles will accelerate at the next time step. Hence, the average speed will decrease with the increase of τ^{CAV}.

As shown in Fig. 9(f), all vehicles with a penetration rate of 100% are in the CACC mode. The vehicles will quickly form a platoon and maintain the maximum speed. At this point, the average speed is not affected by the values of τ^{HDV} and τ^{CAV}.

4.3.3. Maximum platoon size

Maximum platoon size refers to the maximum number of vehicles that can be accommodated in a platoon. A larger platoon size may cause poor traffic flow stabilization, while a small platoon size may cause a waste of capacity. In this

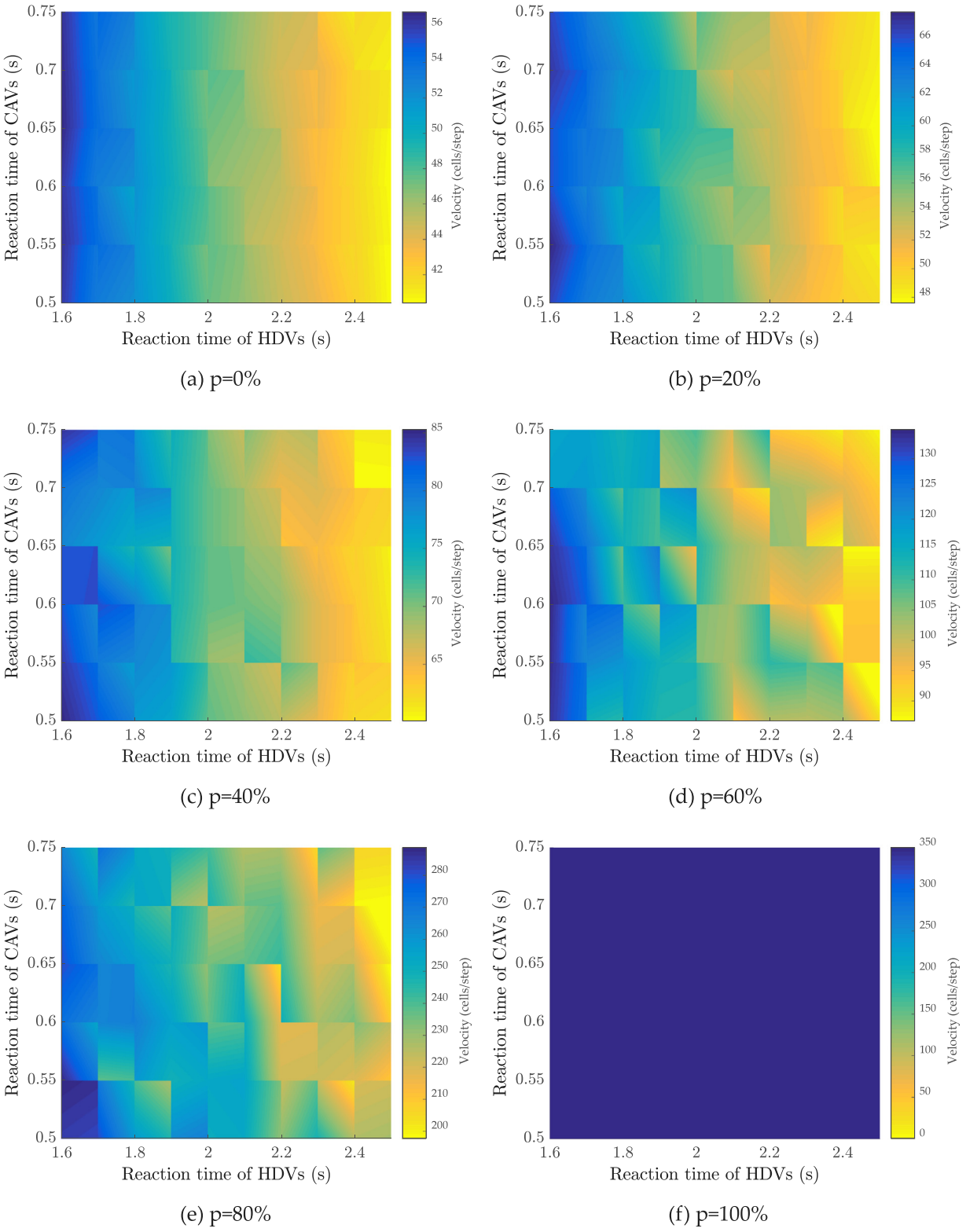

Fig. 9. Sensitivity analysis on reaction time of HDVs and CAVs.

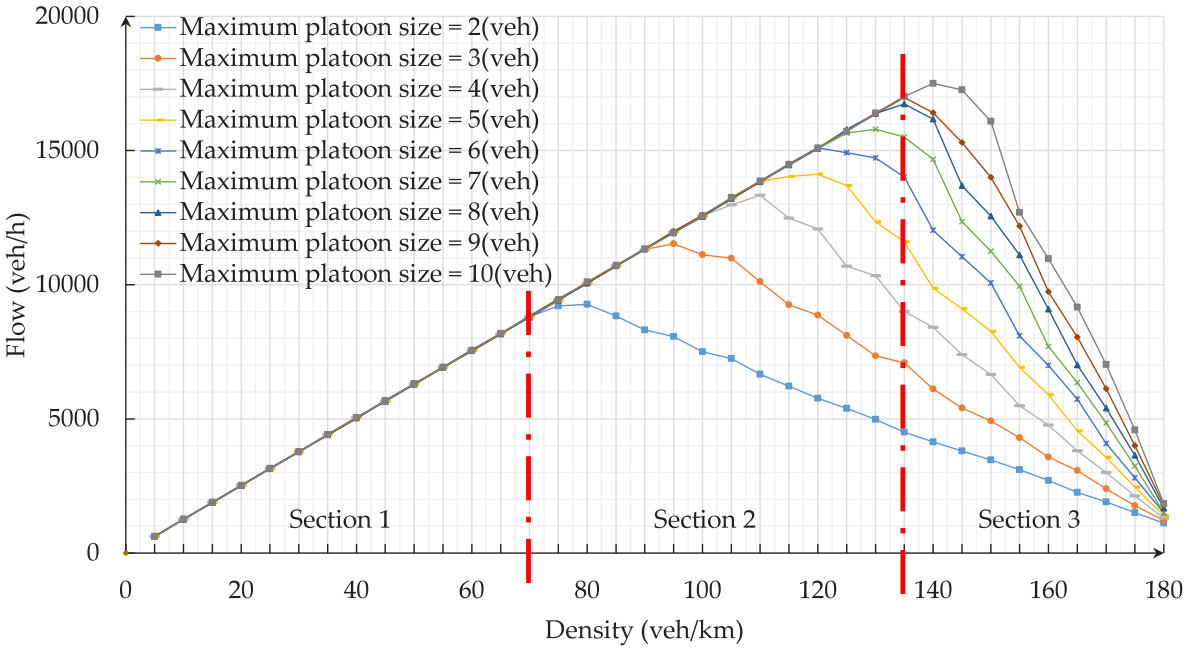

Fig. 10. Sensitivity analysis on maximum platoon size.

sensitivity analysis, the 100% CAVs is selected to discuss the influence of the platoon size. The maximum platoon size varies from 2 to 10 vehs with an increment of 1 veh. The results of sensitivity analysis are shown in Fig. 10.

Fig. 10 shows that a larger maximum platoon size will increase road capacity. The main reason is that the maximum platoon size is inversely proportional to the number of platoons on the road. The decreasing of the average headway will lead to the increase of road capacity with the decrease of platoon number. The impact of maximum platoon size on traffic flow affected by the traffic density can be divided into three sections. Fig. 11 indicates that the curves of each section between the traffic flow and the maximum platoon size.

For section one, the cross-section of density = 40 veh/km is selected to study the effect of maximum platoon size on traffic flow, as shown in Fig. 11(a). The length of the maximum platoon size changes the vehicles' headway, but the vehicle speed remains constant, as vehicles on low-density are in a free flow state. Accordingly, the maximum platoon size has little effect on traffic flow. For section two, the cross-section of density = 100 vehs/km is selected. Fig. 11(b) shows that the traffic flow will increase as the maximum platoon size changes from 2 to 4 vehs before reaching the highest point where the maximum platoon size is 4 vehs and then stay unchanged. Moreover, a small value of maximum platoon size can improve the stabilization of traffic flow [61]. This suggests that there exists an optimal maximum platoon size to maximize the traffic flow and stabilization, which is 4 vehs in this scenario. Because with a small value of maximum platoon size, there will be more vehicles in ACC mode existing on the road. A larger safety distance is required by the vehicles in ACC mode, compared with the vehicles in the platoon. In this section, since the traffic density has reached a relatively large value, the headway is short that not meeting the safety distance requirement of ACC vehicles. In this case, the vehicle will cause deceleration. With the length of maximum platoon size, there will be fewer vehicles deceleration, and the traffic flow will increase. After reaching the optimal maximum platoon size, vehicles will drive in a free flow state that is not affected by the maximum platoon size. For section three, the cross-section of density = 160 veh/km is selected. As shown in Fig. 11(c), the traffic flow will increase continually, and the optimal maximum platoon size does not exist in this figure. The reason is that it will take a considerable length for the platoon in an over-density road to achieve the free flow state. In this section, the optimal maximum platoon size exceeds the 10 vehs.

5. Conclusion and future work

This study proposed a cellular automata model for mixed traffic flow considering the driving behavior of connected automated vehicle platoons. Based on the numerical simulation and sensitivity analysis, the following conclusions are obtained:

(1) The penetration rate of CAVs has a significant impact on road capacity. The road capacity with a penetration rate of 80% is 3.24 times that of only HDVs.

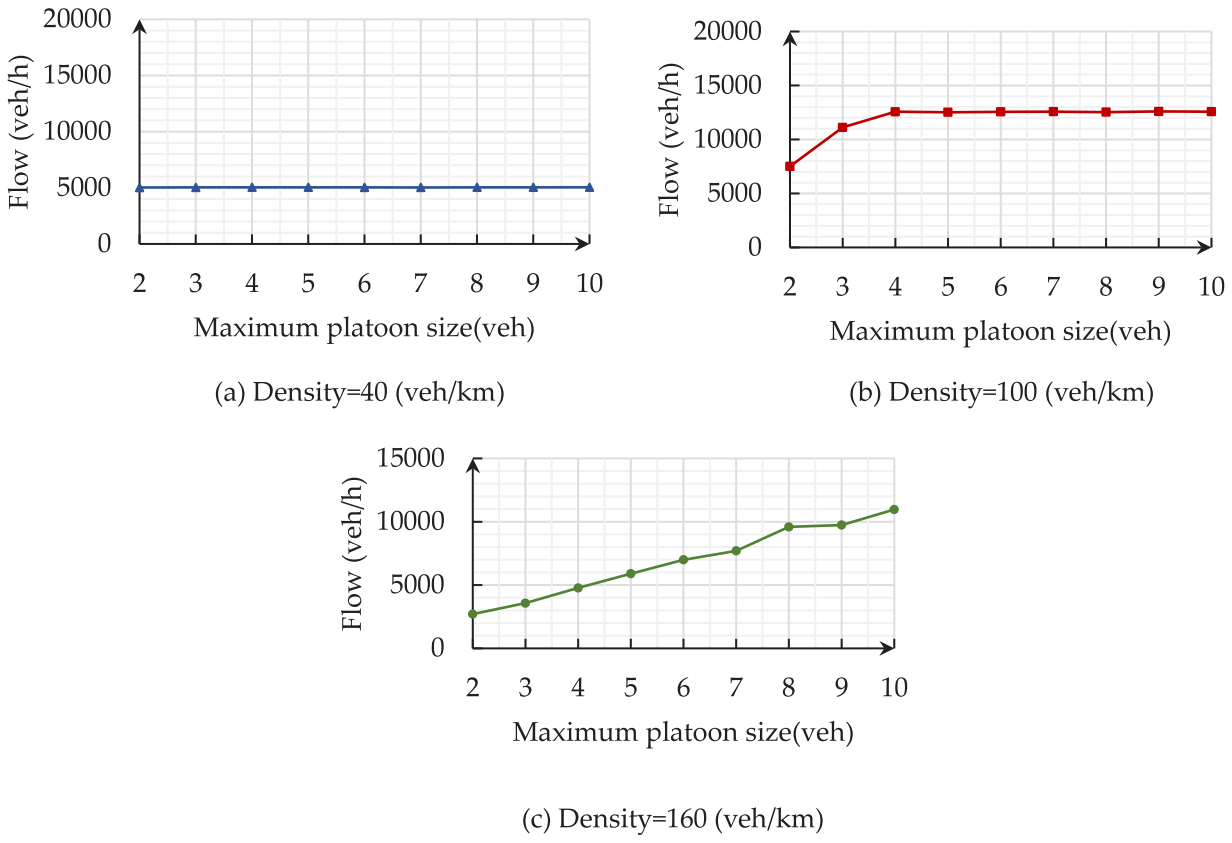

Fig. 11. Flow vs. maximum platoon size of three sections.

(2) The road capacity is only affected by the critical traffic density in the case of penetration rate is 100%, where all the vehicles will drive freely in the form of the platoon.
(3) The average speed of traffic flow decreases with the increase of traffic density. However, under the same traffic density, the average speed can significantly increase with the increase of the penetration rate.
(4) The application of CAVs can effectively alleviate traffic congestion. The congestion reduction percentage can reach 63.36% when the penetration rate of CAVs is 80%.
(5) With the increase of the CAVs penetration rate, the speed volatility will gradually decrease.
(6) The increase of the maximum platoon size will increase the road capacity when the penetration rate of CAVs is 100%. There exists an optimal value of the maximum platoon size when the road density is in an appropriate range.
(7) The safe distance of the vehicles in CACC mode and the reaction time of vehicles will affect the mixed traffic flow. The degree of influence is related to the penetration rate of CAVs and traffic density.

This work only considers the single-lane scene of the freeway rather than the lane-changing rules. In the future, a multi-lane CA model of mixed traffic flow composed of CAVs' platoon will be constructed, where the lane-changing rules will be introduced. Furthermore, the proposed model will be applied to the complex urban traffic environment, which fully considering the impact of intersections, and the characteristics of mixed traffic flow in the factual scene will be further studied.

CRediT authorship contribution statement

Yangsheng Jiang: Data curation, Writing – original draft. **Sichen Wang:** Data curation, Writing – original draft, Visualization, Investigation, Writing – review & editing. **Zhihong Yao:** Conceptualization, Methodology, Software, Supervision, Writing – review & editing. **Bin Zhao:** Visualization, Investigation, Software, Validation. **Yi Wang:** Software, Validation, Writing – review & editing.

Declaration of competing interest

The authors declare that they have no known competing financial interests or personal relationships that could have appeared to influence the work reported in this paper.

Acknowledgments

The paper received research funding support from the National Natural Science Foundation of China (52002339), the Sichuan Science and Technology Program (2021YJ0535, 2020YFH0026), the Fundamental Research Funds for the Central Universities, China (2682021CX058), the Guangxi Science and Technology Program, China (2021AA01007AA), and the Innovation Center Project of Chengdu Jiao Da Big Data Technology Co., Ltd., China (JDSKCXZX202003).

References

[1] Y. Jiang, B. Zhao, M. Liu, Z. Yao, A two-level model for traffic signal timing and trajectories planning of multiple CAVs in a random environment, J. Adv. Transp. 2021 (2021) 1–13, http://dx.doi.org/10.1155/2021/9945398.
[2] Z. Yao, R. Hu, Y. Jiang, T. Xu, Stability and safety evaluation of mixed traffic flow with connected automated vehicles on expressways, J. Safety Res. 75 (2020) 262–274, http://dx.doi.org/10.1016/j.jsr.2020.09.012.
[3] A. Talebian, S. Mishra, Predicting the adoption of connected autonomous vehicles: A new approach based on the theory of diffusion of innovations, Transp. Res. C 95 (2018) 363–380, http://dx.doi.org/10.1016/j.trc.2018.06.005.
[4] Z. Yao, T. Xu, Y. Jiang, R. Hu, Linear stability analysis of heterogeneous traffic flow considering degradations of connected automated vehicles and reaction time, Physica A 561 (2021) 125218, http://dx.doi.org/10.1016/j.physa.2020.125218.
[5] A. Talebpour, H.S. Mahmassani, Influence of connected and autonomous vehicles on traffic flow stability and throughput, Transp. Res. C 71 (2016) 143–163, http://dx.doi.org/10.1016/j.trc.2016.07.007.
[6] M. Treiber, A. Kesting, D. Helbing, Influence of reaction times and anticipation on stability of vehicular traffic flow, Transp. Res. Rec. J. Transp. Res. Board. 1999 (2007) 23–29, http://dx.doi.org/10.3141/1999-03.
[7] Z. Yao, H. Jiang, Y. Cheng, Y. Jiang, B. Ran, Integrated schedule and trajectory optimization for connected automated vehicles in a conflict zone, IEEE Trans. Intell. Transp. Syst. (2020) 1–11, http://dx.doi.org/10.1109/TITS.2020.3027731.
[8] L.C. Davis, Effect of adaptive cruise control systems on traffic flow, Phys. Rev. E 69 (2004) 066110, http://dx.doi.org/10.1103/PhysRevE.69.066110.
[9] A. Kesting, M. Treiber, D. Helbing, Enhanced intelligent driver model to access the impact of driving strategies on traffic capacity, Philos. Trans. R. Soc. Math. Phys. Eng. Sci. 368 (2010) 4585–4605, http://dx.doi.org/10.1098/rsta.2010.0084.
[10] S.E. Shladover, D. Su, X.-Y. Lu, Impacts of cooperative adaptive cruise control on freeway traffic flow, Transp. Res. Rec. J. Transp. Res. Board. 2324 (2012) 63–70, http://dx.doi.org/10.3141/2324-08.
[11] D. Ngoduy, Analytical studies on the instabilities of heterogeneous intelligent traffic flow, Commun. Nonlinear Sci. Numer. Simul. 18 (2013) 2699–2706, http://dx.doi.org/10.1016/j.cnsns.2013.02.018.
[12] W.J. Schakel, B. van Arem, B.D. Netten, Effects of cooperative adaptive cruise control on traffic flow stability, in: 13th Int. IEEE Conf. Intell. Transp. Syst. IEEE, Funchal, Madeira Island, Portugal, 2010, pp. 759–764, http://dx.doi.org/10.1109/ITSC.2010.5625133.
[13] H. Wang, Y. Qin, W. Wang, J. Chen, Stability of CACC-manual heterogeneous vehicular flow with partial CACC performance degrading, Transp. B Transp. Dyn. 7 (2019) 788–813, http://dx.doi.org/10.1080/21680566.2018.1517058.
[14] W. Zhao, D. Ngoduy, S. Shepherd, R. Liu, M. Papageorgiou, A platoon based cooperative eco-driving model for mixed automated and human-driven vehicles at a signalised intersection, Transp. Res. C 95 (2018) 802–821, http://dx.doi.org/10.1016/j.trc.2018.05.025.
[15] W. Hu, L. Yan, H. Wang, Traffic jams prediction method based on two-dimension cellular automata model, in: 17th Int. IEEE Conf. Intell. Transp. Syst. ITSC, IEEE, Qingdao, China, 2014, pp. 2023–2028, http://dx.doi.org/10.1109/ITSC.2014.6958001.
[16] T.-Q. Tang, L. Chen, R.-Y. Guo, H.-Y. Shang, An evacuation model accounting for elementary students' individual properties, Physica A 440 (2015) 49–56, http://dx.doi.org/10.1016/j.physa.2015.08.002.
[17] L.A. Pereira, D. Burgarelli, L.H. Duczmal, F.R.B. Cruz, Emergency evacuation models based on cellular automata with route changes and group fields, Physica A 473 (2017) 97–110, http://dx.doi.org/10.1016/j.physa.2017.01.048.
[18] M.-B. Pang, B.-N. Ren, Effects of rainy weather on traffic accidents of a freeway using cellular automata model, Chin. Phys. B 26 (2017) 108901, http://dx.doi.org/10.1088/1674-1056/26/10/108901.
[19] M. Zamith, R.C.P. Leal-Toledo, E. Clua, E.M. Toledo, G.V.P. de Magalhães, A new stochastic cellular automata model for traffic flow simulation with drivers' behavior prediction, J. Comput. Sci. 9 (2015) 51–56, http://dx.doi.org/10.1016/j.jocs.2015.04.005.
[20] D.N. Dailisan, M.T. Lim, Crossover transitions in a bus–car mixed-traffic cellular automata model, Physica A 557 (2020) 124861, http://dx.doi.org/10.1016/j.physa.2020.124861.
[21] J.H. Zhu, A cellular automata asymmetric lane-changing model with mixed traffic, Adv. Mater. Res. 1030–1032 (2014) 1937–1940, http://dx.doi.org/10.4028/www.scientific.net/AMR.1030-1032.1937.
[22] X. Li, X. Li, Y. Xiao, B. Jia, Modeling mechanical restriction differences between car and heavy truck in two-lane cellular automata traffic flow model, Physica A 451 (2016) 49–62, http://dx.doi.org/10.1016/j.physa.2015.12.157.
[23] D. Yang, X. Qiu, D. Yu, R. Sun, Y. Pu, A cellular automata model for car–truck heterogeneous traffic flow considering the car–truck following combination effect, Physica A 424 (2015) 62–72, http://dx.doi.org/10.1016/j.physa.2014.12.020.
[24] N. Lakouari, K. Bentaleb, H. Ez-Zahraouy, A. Benyoussef, Correlation velocities in heterogeneous bidirectional cellular automata traffic flow, Physica A 439 (2015) 132–141, http://dx.doi.org/10.1016/j.physa.2015.07.024.
[25] D. Kong, L. Sun, J. Li, Y. Xu, Modeling cars and trucks in the heterogeneous traffic based on car–truck combination effect using cellular automata, Physica A 562 (2021) 125329, http://dx.doi.org/10.1016/j.physa.2020.125329.
[26] Q.-L. Li, R. Jiang, J. Min, J.-R. Xie, B.-H. Wang, Phase diagrams of heterogeneous traffic flow at a single intersection in a deterministic fukui-ishibashi cellular automata traffic model, Europhys. Lett. 108 (2014) 28001, http://dx.doi.org/10.1209/0295-5075/108/28001.
[27] K. Bentaleb, N. Lakouari, H. Ez-Zahraouy, A. Benyoussef, Simulation study of satisfaction rate in the mixed traffic flow with open boundary conditions, Internat. J. Modern Phys. C 27 (2016) 1650023, http://dx.doi.org/10.1142/S0129183116500236.
[28] K. Nagel, M. Schreckenberg, A cellular automaton model for freeway traffic, J. Phys. I 2 (1992) 2221–2229, http://dx.doi.org/10.1051/jp1:1992277.
[29] M. Takayasu, H. Takayasu, 1/f noise in a traffic model, Fractals 01 (1993) 860–866, http://dx.doi.org/10.1142/S0218348X93000885.
[30] S.C. Benjamin, N.F. Johnson, P.M. Hui, Cellular automata models of traffic flow along a highway containing a junction, J. Phys. A: Math. Gen. 29 (1996) 3119–3127, http://dx.doi.org/10.1088/0305-4470/29/12/018.

[31] M. Fukui, Y. Ishibashi, Traffic flow in 1D cellular automaton model including cars moving with high speed, J. Phys. Soc. Japan 65 (1996) 1868–1870.
[32] R. Barlovic, L. Santen, A. Schadschneider, M. Schreckenberg, Metastable states in cellular automata for traffic flow, Eur. Phys. J. B 5 (1998) 793–800, http://dx.doi.org/10.1007/s100510050504.
[33] W. Knospe, L. Santen, A. Schadschneider, M. Schreckenberg, Towards a realistic microscopic description of highway traffic, J. Phys. A: Math. Gen. 33 (2000) L477–L485, http://dx.doi.org/10.1088/0305-4470/33/48/103.
[34] X. Li, Q. Wu, R. Jiang, Cellular automaton model considering the velocity effect of a car on the successive car, Phys. Rev. E 64 (2001) 066128, http://dx.doi.org/10.1103/PhysRevE.64.066128.
[35] R. Jiang, Q.-S. Wu, Cellular automata models for synchronized traffic flow, J. Phys. A: Math. Gen. 36 (2002) 381–390, http://dx.doi.org/10.1088/0305-4470/36/2/307.
[36] W.-X. Zhu, H.M. Zhang, Analysis of mixed traffic flow with human-driving and autonomous cars based on car-following model, Physica A 496 (2018) 274–285, http://dx.doi.org/10.1016/j.physa.2017.12.103.
[37] J. Wang, Y. Zheng, Q. Xu, J. Wang, K. Li, Controllability analysis and optimal control of mixed traffic flow with human-driven and autonomous vehicles, IEEE Trans. Intell. Transp. Syst. (2020) 1–15.
[38] D.-F. Xie, X.-M. Zhao, Z. He, Heterogeneous traffic mixing regular and connected vehicles: Modeling and stabilization, IEEE Trans. Intell. Transp. Syst. 20 (2019) 2060–2071, http://dx.doi.org/10.1109/TITS.2018.2857465.
[39] Z. Yao, Y. Wang, B. Liu, B. Zhao, Y. Jiang, Fuel consumption and transportation emissions evaluation of mixed traffic flow with connected automated vehicles and human-driven vehicles on expressway, Energy 230 (2021) 120766, http://dx.doi.org/10.1016/j.energy.2021.120766.
[40] Y. Qin, H. Wang, B. Ran, Stability analysis of connected and automated vehicles to reduce fuel consumption and emissions, J. Transp. Eng. Part Syst. 144 (2018) 04018068, http://dx.doi.org/10.1061/JTEPBS.0000196.
[41] Z. Yao, R. Hu, Y. Jiang, T. Xu, Stability and safety evaluation of mixed traffic flow with connected automated vehicles on expressways, J. Safety Res. 75 (2020) 262–274, http://dx.doi.org/10.1016/j.jsr.2020.09.012.
[42] B. Chen, D. Sun, J. Zhou, W. Wong, Z. Ding, A future intelligent traffic system with mixed autonomous vehicles and human-driven vehicles, Inform. Sci. 529 (2020) 59–72, http://dx.doi.org/10.1016/j.ins.2020.02.009.
[43] Zhang Ning-Xi, Zhu Hui-Bing, Lin Heng, Huang Meng-Yuan, One-dimensional cellular automaton model of traffic flow considering dynamic headway, Acta Phys. Sin. 64 (2015) 024501, http://dx.doi.org/10.7498/aps.64.024501.
[44] X. Hu, M. Huang, J. Guo, Feature analysis on mixed traffic flow of manually driven and autonomous vehicles based on cellular automata, Math. Probl. Eng. 2020 (2020) 1–7, http://dx.doi.org/10.1155/2020/7210547.
[45] T. Vranken, B. Sliwa, C. Wietfeld, M. Schreckenberg, Adapting a cellular automata model to describe heterogeneous traffic with human-driven, automated, and communicating automated vehicles, Physica A 570 (2021) 125792, http://dx.doi.org/10.1016/j.physa.2021.125792.
[46] H.K. Lee, R. Barlovic, M. Schreckenberg, D. Kim, Mechanical restriction versus human overreaction triggering congested traffic states, Phys. Rev. Lett. 92 (2004) 238702, http://dx.doi.org/10.1103/PhysRevLett.92.238702.
[47] D. Yang, X. Qiu, L. Ma, D. Wu, L. Zhu, H. Liang, Cellular automata–based modeling and simulation of a mixed traffic flow of manual and automated vehicles, Transp. Res. Rec. J. Transp. Res. Board. 2622 (2017) 105–116, http://dx.doi.org/10.3141/2622-10.
[48] Y. Liu, J. Guo, J. Taplin, Y. Wang, Characteristic analysis of mixed traffic flow of regular and autonomous vehicles using cellular automata, J. Adv. Transp. 2017 (2017) 1–10, http://dx.doi.org/10.1155/2017/8142074.
[49] H.-T. Zhao, X.-R. Liu, X.-X. Chen, J.-C. Lu, Cellular automata model for traffic flow at intersections in internet of vehicles, Physica A 494 (2018) 40–51, http://dx.doi.org/10.1016/j.physa.2017.11.152.
[50] Y. Liu, X. Lin, F. He, M. Li, Cellular Automata for Modeling Safety Issues in Mixed Traffic of Conventional and Autonomous Vehicles, American Society of Civil Engineers, Reston, VA, 2018.
[51] L. Ye, T. Yamamoto, Evaluating the impact of connected and autonomous vehicles on traffic safety, Physica A 526 (2019) 121009, http://dx.doi.org/10.1016/j.physa.2019.04.245.
[52] T. Muhammad, F.A. Kashmiri, H. Naeem, X. Qi, H. Chia-Chun, H. Lu, Simulation study of autonomous vehicles' effect on traffic flow characteristics including autonomous buses, J. Adv. Transp. 2020 (2020) 1–17, http://dx.doi.org/10.1155/2020/4318652.
[53] W. Wu, Y. Liu, Y. Xu, Q. Wei, Y. Zhang, Traffic control models based on cellular automata for at-grade intersections in autonomous vehicle environment, J. Sens. (2017) 6, http://dx.doi.org/10.1155/2017/9436064.
[54] Y. Jiang, S. Wang, K. Gao, M. Liu, Z. Yao, Cellular automata model of mixed traffic flow composed of intelligent connected vehicles' platoon, J. Syst. Simul. 1–8.
[55] P.G. Gipps, A behavioural car-following model for computer simulation, Transp. Res. B 15 (1981) 105–111, http://dx.doi.org/10.1016/0191-2615(81)90037-0.
[56] J. Zhou, H. Peng, Range policy of adaptive cruise control vehicles for improved flow stability and string stability, IEEE Trans. Intell. Transp. Syst. 6 (2005) 229–237, http://dx.doi.org/10.1109/TITS.2005.848359.
[57] S.E. Shladover, Review of the state of development of advanced vehicle control systems (AVCS), Veh. Syst. Dyn. 24 (1995) 551–595, http://dx.doi.org/10.1080/00423119508969108.
[58] B. Schoettle, Sensor Fusion: A Comparison of Sensing Capabilities of Human Drivers and Highly Automated Vehicles, Univ. Mich., 2017, p. 47.
[59] A. Kesting, M. Treiber, M. Schönhof, D. Helbing, Adaptive cruise control design for active congestion avoidance, Transp. Res. C 16 (2008) 668–683, http://dx.doi.org/10.1016/j.trc.2007.12.004.
[60] R.E. Stern, S. Cui, M.L. Delle Monache, R. Bhadani, M. Bunting, M. Churchill, N. Hamilton, R. Haulcy, H. Pohlmann, F. Wu, B. Piccoli, B. Seibold, J. Sprinkle, D.B. Work, Dissipation of stop-and-go waves via control of autonomous vehicles: Field experiments, Transp. Res. C 89 (2018) 205–221, http://dx.doi.org/10.1016/j.trc.2018.02.005.
[61] J. Zhou, F. Zhu, Analytical analysis of the effect of maximum platoon size of connected and automated vehicles, Transp. Res. C 122 (2021) 102882, http://dx.doi.org/10.1016/j.trc.2020.102882.